International Communications in Heat and Mass Transfer 115 (2020) 104606

Contents lists available at ScienceDirect

International Communications in Heat and Mass Transfer

journal homepage: www.elsevier.com/locate/ichmt

Numerical simulation of heat transfer in a parallel plate channel and promote dissipative particle dynamics method using different weight functions

Marzie Borhani, Somaye Yaghoubi*

[a] Department of Mechanical Engineering, Najafabad Branch, Islamic Azad University, Najafabad, Iran

ARTICLE INFO

Keywords:
Dissipative particle dynamics
Heat transfer
Weight function
Thermal boundary condition
No-slip

ABSTRACT

In this paper heat transfer in a channel with parallel plates has been studied using Dissipative Particle Dynamics with energy conservation (eDPD). To simulate and present different thermal flows in finite geometries, a computer program was developed. The thermal boundary condition of the wall is assumed to be a constant temperature. Each particle in contact with the wall achieves the wall temperature. Also periodic boundary condition in the direction of the flow of the solution domain and no-slip boundary condition on the walls have been considered. The no-slip boundary condition is possible by freezing the layers of particles on the walls and applying bounce-back reflection. The results show dimensionless temperature and velocity profiles perpendicular to the direction of the flow along the channel. Finally, in this research it is tried to endeavored the fluctuations near the wall and promote the method by proposing different weight functions. Four different weight functions were used and the results on the velocity and temperature profiles were investigated. All of the results in the present work were compared and verified with the previous results.

1. Introduction

The combination of numerical methods, consist of repetitive calculations in various applications of physics and ever increasing computation power, play an important role to solve problems in fluid mechanics and heat transfer especially in micro and nano sizes.

For instance, Molecular dynamics (MD) and Lattice Boltzmann Method) LBM) have been used to simulate nanofluids [1,2], slip flow [2,3], nanochannels [4–6] and porous media [7].

In the past decads, DPD method has been used in various applications such as hydrodynamic simulations of suspended particles in a liquid [8–10], complex multi-phase fluids [11–13], polymers [14–17], droplets [18–20] and biology [21,22].

Dissipative Particle Dynamics (DPD) is a particle-based, mesh free simulation method introduced by Hoogerbrugge and Koelman in 1992 to solve hydrodynamic phenomena [23].

This method has been developed by many researchers [24–26]. For instance, Yaghoubi et al. [26] studied improvement of DPD method by considering the particle size. Results demonstrated that using particles with intrinsic size led to the reduction in the required number of particles for simulations. This reduction in the number of particles would result in more economical simulations. According to Abu-Nada's research [27–29] DPD method has been developed to simulate nanofluids heat transfer in a convective system. Majority of the numerical studies reported a significant heat transfer enhancement using nanofluids in convective system. For instance, Abu-Nada et al. [28] presented a novel two-component DPD model to investigate heat transfer enhancement in buoyancy driven flow in a differentially heated cavity using an Al2O3-water nanofluid. Also, Abu-Nada [29] investigated the heat transfer enhancement in a differential heated enclosure filled with a CuO-water nanofluid. The DPD simulations were benchmarked against finite volume method (FVM). The results illustrated that excessive presence of nanoparticles can have a negative effect on heat transfer. Kara et al. [30] reported the effect of Al2O3 nanoparticles on mixed convection heat transfer mechanisms in a vertical lid-driven cavity using DPD method. The results were verified via comparing the temperatures and the streamlines contours with the ones obtained using finite-volume method over the same range of nanoparticles concentration.

The expansion of the isothermal DPD model coupled with its inclusion of the energy equation, has made DPD suitable for simulating different thermal transfer backgrounds. This extended model of eDPD was conducted independently by Avalos & Mackie [31] and Español [32]. Whereas real world engineering and industrial applications, heat

* Corresponding author at: Department of Mechanical Engineering, Najafabad Branch, Islamic Azad University, Najafabad, Iran.
E-mail address: s.yaghoubi@pmc.iaun.ac.ir (S. Yaghoubi).

https://doi.org/10.1016/j.icheatmasstransfer.2020.104606

transfer phenomena often occur in complex geometries, eDPD methods adapt themselves better to simple geometries such as channels, single or two-dimensional containers. This brings the utility of this method to others in simulating complex geometries.

For example, Cao et al. [33] studied numerically the mixed convection flow and heat transfer in eccentric annulus by the eDPD method. The eDPD results for convective heat transfer were compared with the finite volume solutions, lattice Boltzmann method (LBM) and the experimental data. Their results showed a good agreement between them. Zhang et al. [34] developed the eDPD method to simulate fluid-solid conjugate heat transfer in a microchannel. The results by eDPD were mainly benchmarked against those by the FVM for the predictions of heat transfer in a thick-wall microchannel and the eDPD results had good agreement with the predictions of FVM. Results approved that the eDPD method is suitable for conjugating heat transfer in complex geometry. In another work, Yamada et al. [35] studied the forced convection heat transfer in parallel–plate channels using eDPD method. The Simulation was performed for a two–dimensional channel with periodic and no-slip boundary conditions. The eDPD method was benchmarked by comparing the Nusselt number of the numerical results. The Nusselt numbers for two thermal boundary conditions, constant wall temperature (CWT), and constant wall heat flux (CHF) were calculated. The results were verified via comparing the exact solution within 2.3%.

This study simulates forced convective heat transfer in the flow in a channel with parallel plate, using eDPD and modeling different streams. The governing equations for the conservation of momentum and energy are considered based on fully developed thermal and hydrodynamic conditions. Constant temperature is considered for the walls as thermal boundary condition. To study the heat transfer behavior of the channel, two wall conditions were considered, i.e. the same and different wall temperatures.

As DPD method roughly is a new numerical method, there are some deficiencies with this method. To promote that, different researchers have tried to solve them some deal. In this paper, we also endeavored in this field and compared different weight functions in DPD to obviate some depletions in this method.

The paper is organized as follows. In Section 2 we will introduce the eDPD governing equations. In Section 3, the results of the simulation of eDPD for the channel with parallel plates will be shown and the effect of different weighting functions will be investigated. The conclusions will be given in Section 4.

2. Methodology

2.1. Governing equations

In this section, the eDPD model is introduced. The forces in the DPD method include three parts: conservative force $\overrightarrow{F}_{ij}^{C}$, dissipative force $\overrightarrow{F}_{ij}^{D}$ and random force $\overrightarrow{F}_{ij}^{R}$ [35]:

$$\overrightarrow{F}_{ij}^{C} = F^{C}{}_{ij}(r_{ij})\overrightarrow{e}_{ij} \tag{1}$$

$$\overrightarrow{F}_{ij}^{D} = -\gamma_{ij} w^{D}(r_{ij})(\overrightarrow{e}_{ij}.\ \overrightarrow{v}_{ij})\overrightarrow{e}_{ij} \tag{2}$$

$$\overrightarrow{F}_{ij}^{R} = \sigma_{ij} w^{R}(r_{ij})\,\xi_{ij}\Delta t^{-1/2}\overrightarrow{e}_{ij} \tag{3}$$

where $\overrightarrow{e}_{ij} = \overrightarrow{r}_{ij}/r_{ij}$ is a unit vector in the direction between particles i and j. Also $\overrightarrow{r}_{ij} = \overrightarrow{r}_i - \overrightarrow{r}_j$ and $\overrightarrow{v}_{ij} = \overrightarrow{v}_i - \overrightarrow{v}_j$. Conservative force F^C shows the effect of particles on each other in real mode (non-ideal). In these systems, each particle will react only to its neighboring particles. The random forces within the DPD system are controlled by r_{ij}. In the eDPD method, conservation laws are governed on the movement of particle. The i-th particle motion equation is defined according to the following equations [35]:

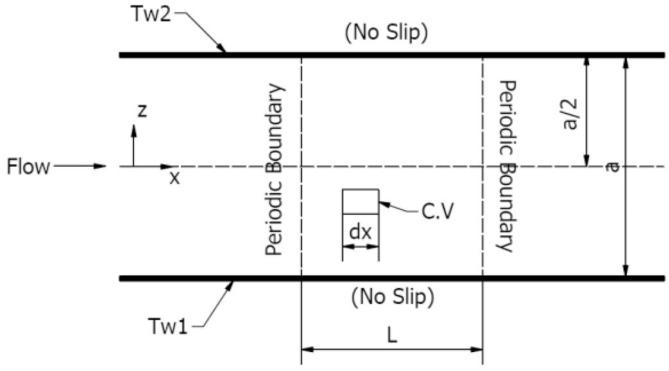

Fig. 1. Schematic of the problem geometry.

Table 1
eDPD parameters.

ρ	a_{ij}	γ_{ij}	r_C	C_V	k_0
4	18.75	4.5	1.0	1.0×10^5	1.26×10^{-4}

$$\frac{d\overrightarrow{r_i}}{dt} = \overrightarrow{v_i} \tag{4}$$

$$m_i \frac{d\overrightarrow{v_i}}{dt} = \overrightarrow{f_i} = \overrightarrow{f}_i^{int} + \overrightarrow{f}_i^{ext} \tag{5}$$

where $\overrightarrow{r_i}$ and $\overrightarrow{v_i}$ describe the position and velocity of the particle, respectively. m_i is the mass i-th particle, $\overrightarrow{f}_i^{ext}$ is the externally force applied such as gravity, and $\overrightarrow{f}_i^{int}$ is presented by:

$$\overrightarrow{f}_i^{int} = \sum_{\substack{i\neq j \\ j=1}}^{N} \overrightarrow{F_{ij}} = \sum_{\substack{i\neq j \\ j=1}}^{N} (\overrightarrow{F}_{ij}^{C} + \overrightarrow{F}_{ij}^{D} + \overrightarrow{F}_{ij}^{R}) \tag{6}$$

where N is the total DPD particles in the domain, $\overrightarrow{F_{ij}}$ represents the inter-particle force on particle i from all other N-1 particles, such that $\overrightarrow{F_{ij}} = \overrightarrow{F_{ji}}$. Because all the forces in this method have a dual nature like action and reaction, the law of linear conservation of momentum will be established. On the other hand, due to the constant number of system particles in the simulation step, the conservation of mass is also satisfied. In the eDPD method, due to the allocation of temperature T_i to the i-th, it is necessary to maintain the law of conservation of energy. This equation is presented as follows [35]:

$$C_v \frac{dT_i}{dt} = q_i \tag{7}$$

where C_v is the heat capacity of DPD particles at constant volume. Generally, the heat capacity of DPD particles is presented dimensionless. This means that $\overline{C_v} = {C_v}/{k_B}$.Where k_B is Boltzmann's constant. Also q_i is the heat flux between particles and includes three parts: viscous, conductive and random heat fluxes. Thus, it can be written:

$$q_i = \sum_{\substack{i\neq j \\ j=1}}^{N} q_{ij} = \sum_{\substack{i\neq j \\ j=1}}^{N} (q_{ij}^{visc} + q_{ij}^{cond} + q_{ij}^{R}) \tag{8}$$

where the first term is related to the viscous heat flux, the second term represents the conduction flux, and the last term is related to the random heat flux. It should be noted that the sum runs over all other particles within a certain cut-off radius r_C [36,37]. Similarly, the expression q_i can be written as follows:

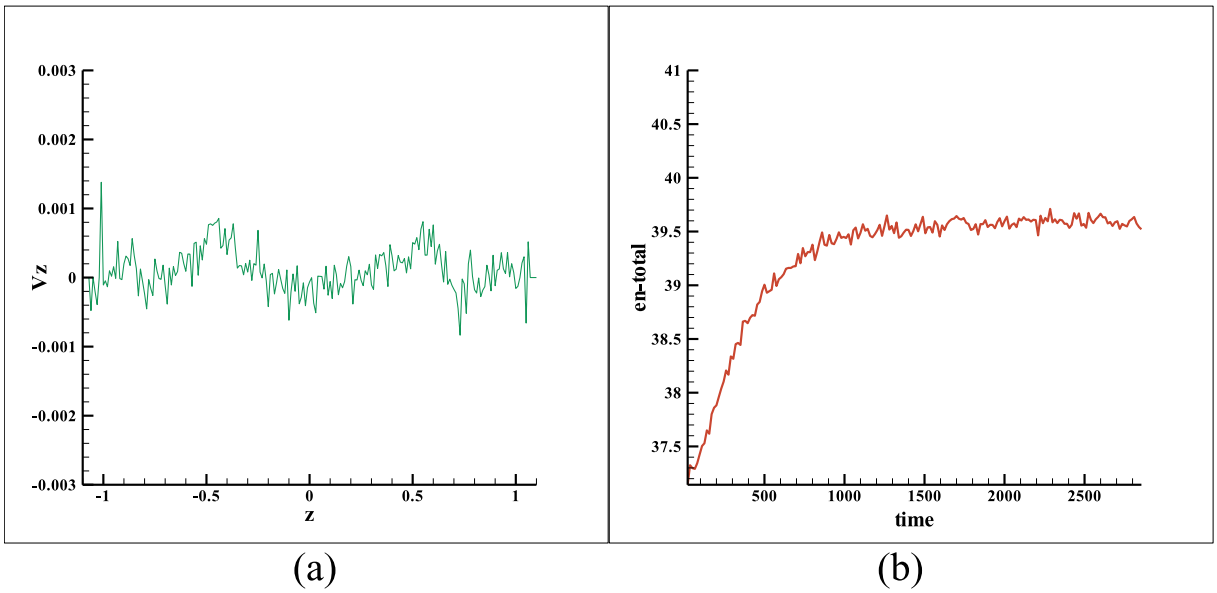

Fig. 2. a) Velocity in z direction and hydrodynamic fully developed flow, and b) total energy changes versus to time.

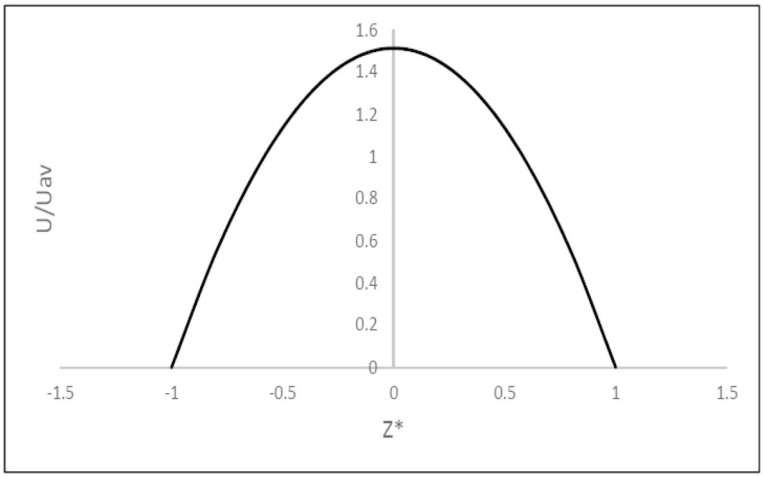

Fig. 3. Dimensionless Velocity profile using CFD modeling.

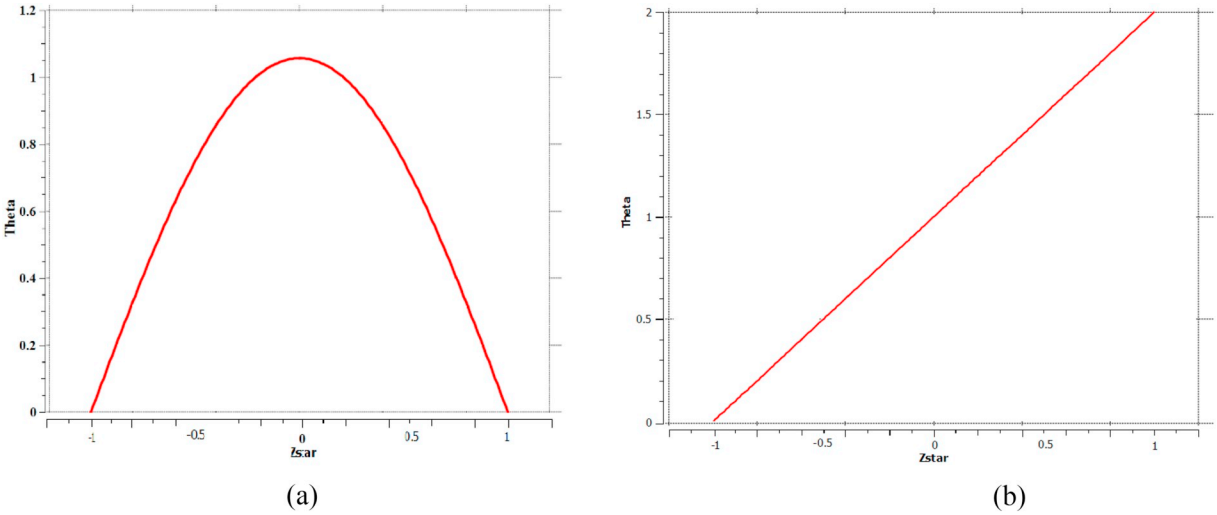

Fig. 4. Dimensionless temperature difference profile using CFD modeling a) Two walls at the same constant temperature, and b) Top and bottom walls at different constant temperature.

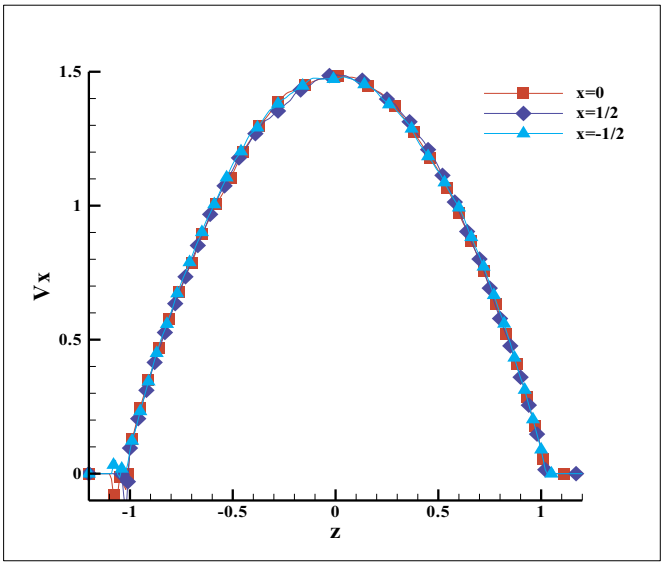

Fig. 5. The velocity profile across the channel cross- Sections ($\mathbf{x} = -\frac{1}{2}, \mathbf{0}, \frac{1}{2}$).

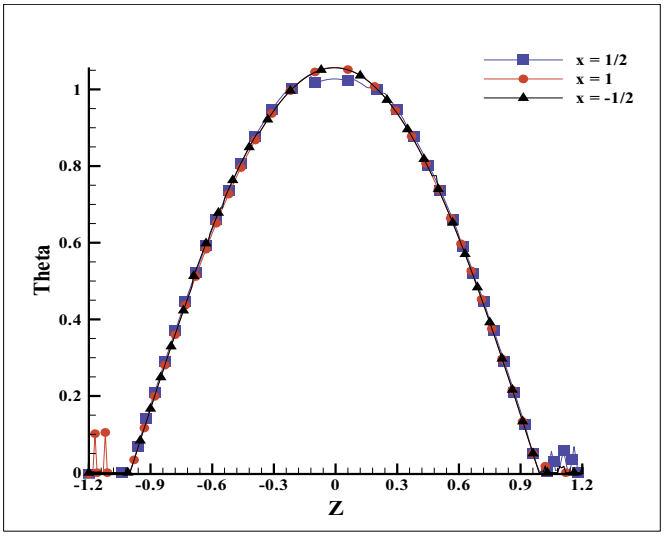

Fig. 6. The dimensionless temperature difference profile across the channel in some cross- Sections ($\mathbf{x} = -\frac{1}{2}, \mathbf{0}, \frac{1}{2}$) with the same wall temperature.

$$q_i = \sum_{\substack{i \neq j \\ j=1}}^{N} \left[\left(\frac{1}{2C_v} \left(w^D(r_{ij}) \left[\gamma_{ij} (\vec{e}_{ij}.\ \vec{v}_{ij})^2 - \frac{{\sigma_{ij}}^2}{m_i} \right] - \sigma_{ij} w^R(r_{ij}) (\vec{e}_{ij}.\ \vec{v}_{ij}) \xi_{ij} \right) \right) + \left(\kappa_{ij} w^2(r_{ij}) \left(\frac{1}{T_i} - \frac{1}{T_j} \right) \right) + \left(\alpha_{ij} w^R(r_{ij}) \Delta t^{-\frac{1}{2}} \xi_{ij}^{e} \right) \right] \tag{9}$$

where ${\xi_{ij}}^e$ is a random number with unit variance and a zero mean. Each pair of DPD particles in the equilibrium obtains a value of ${\xi_{ij}}^e$ such that ${\xi_{ij}}^e = -{\xi_{ji}}^e$. It can be seen that velocity is also involved in the viscous heat flux and cannot be obtained directly from one another. On the other hand, conduction flux depends on temperature and will not be obtained independently.The modified velocity Verlet algorithm predict and correct the solution is used to solve the conservative equations, find the location, velocity, temperature and also heat flux transmitted and force applied to each particle.

All of the weight functions decrease monotonically with the increase of the particle–particle separation distance. In this study, several weight functions are adopted and compared, which are given as:

The classic weight function [33]:

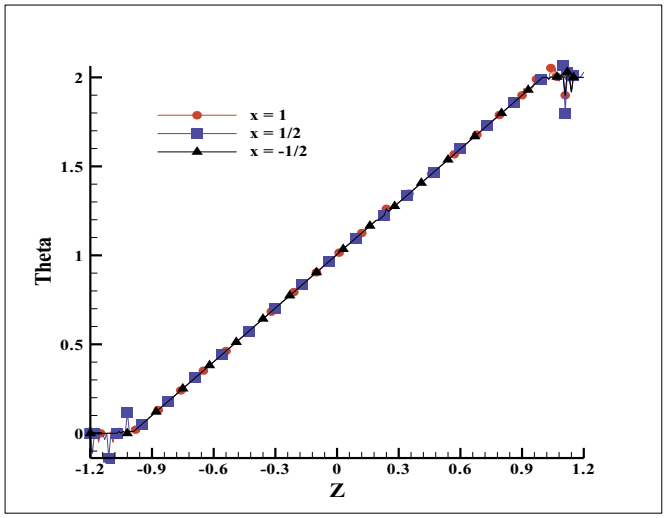

Fig. 7. The dimensionless temperature difference across the channel in some cross- Sections ($\mathbf{x} = -\frac{1}{2}, \mathbf{0}, \frac{1}{2}$) with different wall temperatures.

$$\omega^D(r) = (\omega^R(r))^2 = \begin{cases} 1 - \dfrac{r_{ij}}{r_C} & r_{ij} \leq r_C \\ 0 & r_{ij} > r_C \end{cases} \tag{10}$$

The Fan et al. weighing function [38]:

$$\omega^D(r) = (\omega^R(r))^2 = \begin{cases} \left(1 - \dfrac{r_{ij}}{r_C}\right)^s & r_{ij} \leq r_C \\ 0 & r_{ij} > r_C \end{cases} \tag{11}$$

Here, s is the exponent of the weight functions. As described in Ref. [34] the standard value, $s = 0.25$, is used.

Yaghoubi et al. weight function [39]:

$$\omega^D(r) = (\omega^R(r))^2 = \begin{cases} 1 - \left(\dfrac{r_{ij}}{r_C}\right)^k & r_{ij} \leq r_C \\ 0 & r_{ij} > r_C \end{cases} \tag{12}$$

According to their results, for more accurate modeling of the Schmidt number (Sc), it is necessary to use large quantities for k as the exponent of the weight functions. In this study k is chosen to be 60.

Lucy's weight function [35]:

The Lucy's weight function is widely used in heat transfer simulations, which can be written as: [35,40]:

$$\omega^R(r) = \begin{cases} \dfrac{5}{\pi} \left(1 + 3\dfrac{r_{ij}}{r_C}\right) \left(1 - \dfrac{r_{ij}}{r_C}\right)^3 & r_{ij} \leq r_C \\ 0 & r_{ij} > r_C \end{cases} \tag{13}$$

The parameters γ_{ij} and σ_{ij} is presented by the Fluctuation Dissipation theorem [37,41–43].

$$\gamma = \frac{\sigma^2 (T_i + T_j)}{4 k_B T_i T_j} \tag{14}$$

κ_{ij} and α_{ij} are conductive heat flux and coefficient of random forces, respectively. These coefficients are obtained by the following correlations [35]:

$$\kappa_{ij} = \frac{C_v^2 k_0 (T_i + T_j)^2}{4 k_B} \tag{15}$$

$$\alpha_{ij} = \sqrt{2 k_B \kappa_{ij}} \tag{16}$$

where k_B is the Boltzmann's constant and k_0 is interpreted as heat friction that controls thermal conductivity [36]. k_0 is constant value; indeed, it is regulated by comparing the results of this method with

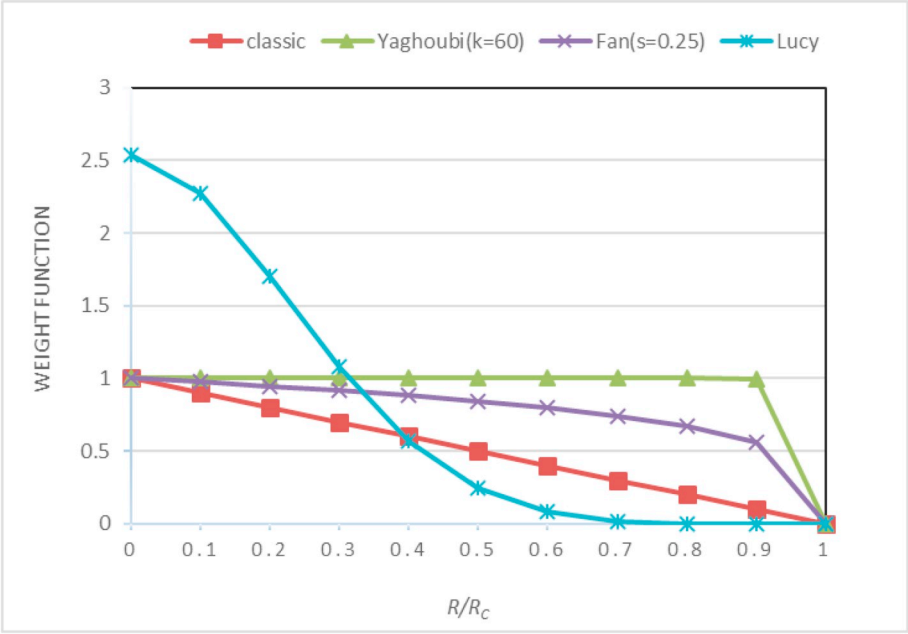

Fig. 8. Comparison of different weight functions in DPD as a function of r/r_c.

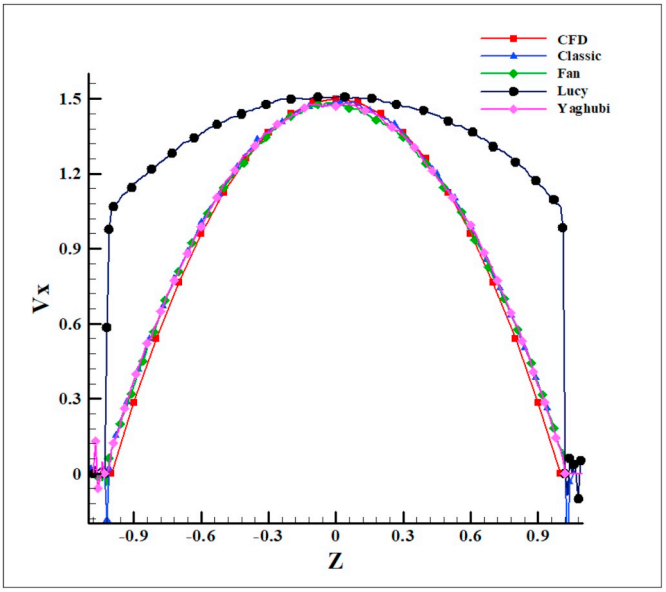

Fig. 9. Comparison of the velocity profile with the different weight function.

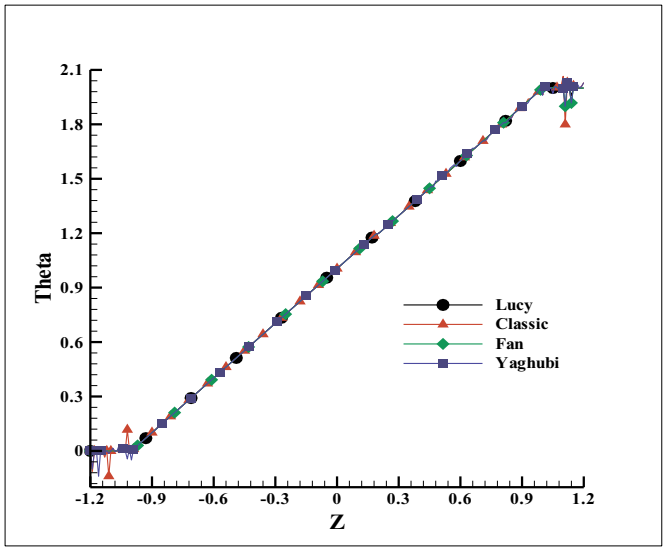

Fig. 10. Comparison of the dimensionless temperature difference with different weight functions, (channel with different wall temperatures).

finite volume methods for the desired geometry.

Since the DPD method has short-range forces and heat fluxes, it is sufficient to calculate the force and heat flux on a particle to examine the particles in the neighborhood of that particle at each time step. Neighboring particles mean the particles located within the radius r_c of the goal particle. For this purpose, the search algorithms have been used to find particles located in the neighborhood. In this paper, the cell list algorithm is used. In this algorithm, it is only necessary to calculate the interactions of the right and top cells of the target particle and compute the values obtained from the interactions of the left and bottom directions previously calculated in the other cells.

2.2. Boundary conditions

The bounce back reflection is used to apply the no-slip boundary condition; in which it is assumed that the particle returns to the fluid domain again in the opposite direction of the inlet path. In other words, both the tangential component and the vertical component of velocity are reversed:

$$(V_n)_{After\ Collision} = -V_n \tag{17}$$

$$(V_t)_{After\ Collision} = -V_t$$

The dimensionless temperature for the case of constant wall temperature boundary condition is expressed as [36]:

$$\theta = \frac{T - T_w}{T_m - T_w} \tag{18}$$

where T_w is the wall temperature, T is the localized fluid temperature and T_m is the average fluid temperature at the cross section. The average temperature can also be calculated by the following correlation [44]:

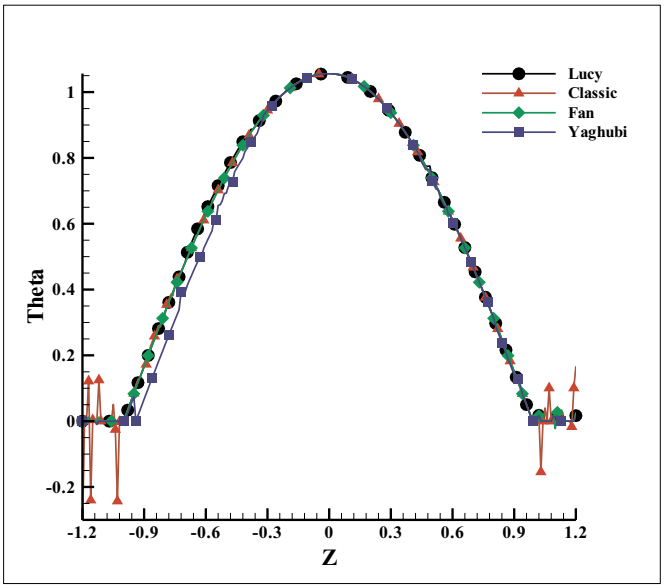

Fig. 11. Comparison of the dimensionless temperature difference with different weight functions, (channel with the same wall temperatures).

$$T_m - T_w = \frac{\int_{Ac} (T - T_w) u dz}{\int_{Ac} u dz} \tag{19}$$

To apply the fully developed hydrodynamic condition, it is sufficient to use the periodic boundary condition at the input and output of the channel. In this case, periodic flow boundary conditions are applied on the fluid boundary of the computational domain in the x and y directions. With that interpretation, the particles move out of the solution domain re-enter the domain with the same position and velocity. For the same wall temperature boundary condition, the dimensionless temperature satisfies the following correlation [35].

$$\theta(x,z) = \theta(x + l,z) = \theta(x + 2l,z) = \ldots \tag{20}$$

Therefore, the temperature field in the fully developed region repeats itself in the intervals l. The derivative of the dimensionless temperature difference relative to time, leads to the following equation:

$$\frac{d\theta}{dt} = \frac{1}{T_m - T_w}\frac{dT}{dt} + \frac{T - T_w}{(T_m - T_w)^2}\frac{dT_m}{dt} \tag{21}$$

In the fully developed temperature regime, $\frac{dT_m}{dt} = 0$, as a result $\frac{dT}{dt}$ can be achieved by rewriting the Eq. (20):

$$\frac{dT}{dt} = (T_m - T_w)\frac{d\theta}{dt} \tag{22}$$

By integrating Eq. (22) into Eq. (7), the modified equation for the state of the same wall temperature is expressed as [35]:

$$\frac{d\theta}{dt} = \frac{1}{C_v(T_m - T_w)}(q_{ij}^{visc} + q_{ij}^{cond} + q_{ij}^{R}) \tag{23}$$

2.3. Forced convection heat transfer problems

A schematic of the problem geometry is shown in Fig. 1, which consists of flow and temperature boundary conditions. As shown in the Fig. 1, the flow with applied force $F_{ext} = 0.01$ enters in the channel by using periodic boundary. The channel dimensions along x and z are $L = 5$ and $a = 40$, respectively. The no-slip boundary condition is possible by freezing the layers of particles on the walls and applying bounce-back reflection. The number of particles needed for wall and fluid domain modeling is 800 and 4000 DPD particles, respectively. The no-slip boundary condition for the velocity is imposed on the surfaces and the fully developed conditions are widely adopted. The temperature condition on the walls is constant temperature, and three different modes have been investigated:

1- The upper and lower wall temperatures are considered to be 1.2 and 0.8, respectively, in DPD units.
2- The upper and lower wall temperatures are equal and considered 1.2 DPD units.
3- Both of the wall temperatures are equal 0.8 DPD units.

The DPD parameters used are given in Table 1 [35].

3. Results and discussion

3.1. Validation of the methodology

In Fig. 2(a), the velocity component has been shown in the z-direction. As it is obvious in the figure, some minor fluctuations can be seen around the value 0 that could be ignored because a statistical method is being used. The energy parameters have been controlled to achieve stability. The stability condition for the system is that the level of the energy remains unchanged during the time. As it can be seen in Fig. 2(b), the changes in the total energy is negligible. It has become almost a constant linear since the time $t = 1000\ s$ which indicates the stability of the problem. It is important to say that the eDPD results presented in this section are obtained using the classic weight function.

Figs. 3 and 4 show the dimensionless velocity and temperature difference profile using CFD modeling as a reference for comparing eDPD results.

Fig. 5 shows the dimensionless velocity profile across the channel in several cross-sections ($\mathbf{x} = -\frac{1}{2}, \mathbf{0}, \frac{1}{2}$) that has acceptable conformity with each other.

In Fig. 6, the profile of the dimensionless temperature difference has been drawn for a state where the temperature of the top and bottom walls of the channel are equal. The temperature has been determined as 1.2 in DPD unit.

In Fig. 7, the profile has been drawn for the state where the temperature of the bottom wall of the channel has been selected 0.8 and that the top wall of the channel has been determined 1.2. As it can be seen, if the temperature of the walls is not equal, the conduction heat transfer term will be very powerful and it will dominate the forced convection heat transfer.

As shown in the results of the eDPD and CFD method, the CFD solution presents from -1 to $+1$, while in eDPD solutions, more thickness is considered at the beginning and the end of the vertical cross-section of the channel. This difference is due to the modification of the walls by freezing the particles in the eDPD method. In fact, ± 0.2 represents the thickness of the walls.

3.2. Promote DPD method near the wall using different weight functions

One of the deficiencies attributed to the DPD method is about the simulation behavior when applying boundary conditions near the wall because of the fluctuations sometimes with high amplitude. In this section, it is attempted to investigate the effect of different weight functions in DPD simulations for boundary conditions near the wall.

In order to analyze them better, the behavior of the weight functions which introduced before versus to the inter-particle distances are depicted in Fig. 6. In this figure, the details of the behavior of these functions will be compared more exactly based on the inter-particle distances.

As it can be seen in Fig. 8, Fan and specially Yaghoubi weight functions will be able to predict the dissipative force to a great extent for many particles with a vast expanse of inter-particle distances, while Lucy weight function can predict the dissipative force to a great extent only for the particles that are very close to each other. It can be

observed that the classic weight function predicts less dissipative force in comparison with Fan and Yaghoubi weight functions. This is the case where this classic weight function predicts a less dissipative force than the Lucy weight function only in the inter-particle distances of about 40% of cut-off radius, and we observe a sharp drop in Lucy weight function even in comparison with the classic one in case of the inter-particle distances greater than 40% of cut-off radius.

As it can be seen in Fig. 9, Lucy's weight function has obviously caused sliding on the wall. In other words, the flow has slid near the wall using this function because of the low viscosity. Despite the success of this function in estimating the maximum velocity, it is not recommended employing this function to conduct a hydrodynamic analysis of the flow. The classic weight function is almost in good agreement with the analytical solution; however, some fluctuations have been observed near the wall. The Fan and Yaghoubi weight functions have controlled the fluctuations near the wall largely by modifying the viscosity.

In the following the dimensionless temperature difference profile with the above introduced weight functions have been drawn for two states. The first one in Fig. 10 is for the case in which the channel walls have different temperatures. As it can be seen in this diagram, almost all weight functions have simulated the inter-particle heat conduction eDPD well. In this regard, Lucy's weight function performs better and its results are in good agreement with the analytical solution. The classic weight function near the walls has undergone some minor fluctuations. The second state in Fig. 11 has been drawn that the walls of the channel have equal temperatures. The temperature of the walls has been determined as 0.8. Again, it can be observed in this diagram that the conformity of the simulation with Lucy weight function is greater than the other weight functions. Also, some minor fluctuations near the wall were observed for the simulations which used Fan and Yaghoubi weight functions which are negligible. More fluctuations have been observed in the case with classic weight function.

According to Fig. 8 which illustrated a comparison between the behaviors of different weight functions in the inter-particle distances, it is obvious the greatest amount of viscosity and then the random fluctuations is provided by Lucy's weight function in comparison with those of other weight functions but only for limited inter particle distances. It can be pointed out to interpret the temperature results, that is, the random force using this weight function in these limited inter particle distances will provide an amount more than twice one which provided by other weight functions. As for the classic weight function in these limited inter particle distances, this amount has decreased considerably in relation to those of Fan and Yaghoubi weight functions.

4. Conclusion

In this research, the heat transfer in a parallel plate channel with constant wall temperature condition was investigated by DPD method. Assuming the temperature for each DPD particle, the heat flux term involved in the conservation of energy equation was correctly simulated. To study the heat transfer behavior of the channel, two conditions were considered, different and the same wall temperature. To apply the developed heat condition to the periodic boundaries, the law of conservation of energy was rewritten in terms of the dimensionless temperature difference.

At each time step, the DPD particle temperature is calculated from this dimensionless temperature difference, and then heat flux will be calculated.

Also, using different weight functions and comparing their behavior in terms of inter particle distances, we have obtained very important results regarding the fluctuations of this numerical method for the velocity diagrams and the dimensionless temperature difference near the wall. As we know, these fluctuations are considered as the major challenges of the DPD method near the wall.

According to the investigations, it is found Yaghoubi and Fan weight functions can control the fluctuations near the wall in velocity and temperature diagrams better than the classic one. Also Lucy weight function is a very good choice for temperature simulation.

References

[1] A. Karimipour, M. Hemmat Esfe, R. Safaei, D. Toghraie Semiromi, S. Jafari, S.N. Kazi, Mixed convection of copper–water nanofluid in a shallow inclined lid driven cavity using the lattice Boltzmann method, Physica A 402 (2014) 150–168, https://doi.org/10.1016/j.physa.2014.01.057.

[2] A. Karimipour, A. Hossein Nezhad, A. D'Orazio, M. Hemmat Esfe, R. Safaei, E. Shirani, Simulation of copper–water nanofluid in a microchannel in slip flow regime using the lattice Boltzmann method, Eur. J. Mech. B Fluids 49 (A) (2015) 89–99, https://doi.org/10.1016/j.euromechflu.2014.08.004.

[3] A. D'Orazio, A. Karimipour, A useful case study to develop lattice Boltzmann method performance: gravity effects on slip velocity and temperature profiles of an air flow inside a microchannel under a constant heat flux boundary condition, Int. J. Heat Mass Transf. 136 (2019) 1017–1029, https://doi.org/10.1016/j.ijheatmasstransfer.2019.03.029.

[4] P. Alipour, D. Toghraie, A. Karimipour, M. Hajian, Modeling different structures in perturbed Poiseuille flow in a nanochannel by using of molecular dynamics simulation: study the equilibrium, Physica A 515 (2019) 13–30, https://doi.org/10.1016/j.physa.2018.09.177.

[5] L. Hantao, L. Yuxiang, J. Shan, C. Jianzhong, H. Haijin, Energy-conserving dissipative particle dynamics simulation of macromolecular solution flow in microchannel under thermal convection, Eng. Anal. Bound. Elem. 102 (2019) 21–28, https://doi.org/10.1016/j.enganabound.2019.02.006.

[6] S. Jafari, R. Zakeri, M. Darbandi, DPD simulation of non-Newtonian electroosmotic fluid flow in nanochannel, Mol. Simul. 44 (17) (2018) 1444–1453, https://doi.org/10.1080/08927022.2018.1517414.

[7] A. Zarei, A. Karimipour, A. Meghdadi Isfahani, Z. Tian, Improve the performance of lattice Boltzmann method for a porous nanoscale transient flow by provide a new modified relaxation time equation, Physica A 535 (2019) 122453, https://doi.org/10.1016/j.physa.2019.122453.

[8] Z. Li, G. Drazer, Hydrodynamic interactions in dissipative particle dynamics, Phys. Fluids 20 (10) (2008) 103601, https://doi.org/10.1063/1.2980039.

[9] R. Qiao, P. He, Mapping of dissipative particle dynamics in fluctuating hydrodynamics simulations, J. Chem. Phys. 128 (12) (2008) 126101, https://doi.org/10.1063/1.2897991.

[10] D.S. Bolintineanu, G.S. Grest, J.B. Lechman, F. Pierce, S.J. Plimpton, P.R. Schunk, Particle dynamics modeling methods for colloid suspensions, Comput. Part. Mech. 1 (3) (2014) 321–356, https://doi.org/10.1007/s40571-014-0007-6.

[11] Mou-Bin Liu, Jian-Zhong Chang, Han-Tao Liu, DPD simulation of multiphase flow at small scales, 2010 The 2nd International Conference on Computer and Automation Engineering (ICCAE), IEEE, 2010, , https://doi.org/10.1109/iccae.2010.5451423.

[12] M. Liu, P. Meakin, H. Huang, Dissipative particle dynamics simulation of multiphase fluid flow in microchannels and microchannel networks, Phys. Fluids 19 (3) (2007) 33302, https://doi.org/10.1063/1.2717182.

[13] M. Liu, P. Meakin, H. Huang, Dissipative particle dynamics simulation of pore-scale multiphase fluid flow, Water Resour. Res. 43 (4) (2007), https://doi.org/10.1029/2006wr004856.

[14] S. Litvinov, Q. Xie, X. Hu, N. Adams, M. Ellero, Simulation of individual polymer chains and polymer solutions with smoothed dissipative particle dynamics, Fluids 1 (1) (2016) 7, https://doi.org/10.3390/fluids1010007.

[15] K. Yang, A. Vishnyakov, A.V. Neimark, Polymer translocation through a nanopore: DPD study, J. Phys. Chem. B 117 (13) (2013) 3648–3658, https://doi.org/10.1021/jp3104672.

[16] M. Jehser, G. Zifferer, C. Likos, Scaling and interactions of linear and ring polymer brushes via DPD simulations, Polymers 11 (3) (2019) 541, https://doi.org/10.3390/polym11030541.

[17] G. Kacar, Dissipative particle dynamics simulation parameters and interactions of a hydrogel, J. Turk. Chem. Soc. Chem. (2017) 19–38, https://doi.org/10.18596/jotcsa.309646.

[18] D. Pan, N. Phan-Thien, B.C. Khoo, Dissipative particle dynamics simulation of droplet suspension in shear flow at low capillary number, J. Non-Newtonian Fluid Mech. 212 (2014) 63–72, https://doi.org/10.1016/j.jnnfm.2014.08.011.

[19] D. Pan, N. Phan-Thien, B.C. Khoo, Studies on liquid–liquid interfacial tension with standard dissipative particle dynamics method, Mol. Simul. 41 (14) (2014) 1166–1176, https://doi.org/10.1080/08927022.2014.952636.

[20] Y. Zhang, J. Xu, X. He, Effect of surfactants on the deformation of single droplet in shear flow studied by dissipative particle dynamics, Mol. Phys. 116 (14) (2018) 1851–1861, https://doi.org/10.1080/00268976.2018.1459916.

[21] M. Basan, J. Prost, J.-F. Joanny, J. Elgeti, Dissipative particle dynamics simulations for biological tissues: rheology and competition, Phys. Biol. 8 (2) (2011) 26014, https://doi.org/10.1088/1478-3975/8/2/026014.

[22] T. Ye, N. Phan-Thien, B.C. Khoo, C.T. Lim, Dissipative particle dynamics simulations of deformation and aggregation of healthy and diseased red blood cells in a tube flow, Phys. Fluids 26 (11) (2014) 111902, https://doi.org/10.1063/1.4900952.

[23] P.J. Hoogerbrugge, J.M.V.A. Koelman, Simulating microscopic hydrodynamic phenomena with dissipative particle dynamics, EPL 19 (3) (1992) 155–160, https://doi.org/10.1209/0295-5075/19/3/001.

[24] N. Phan-Thien, N. Mai-Duy, T.Y.N. Nguyen, A note on dissipative particle dynamics (DPD) modelling of simple fluids, Comput. Fluids 176 (2018) 97–108, https://doi.org/10.1016/j.compfluid.2018.08.030.

[25] N. Mai-Duy, N. Phan-Thien, T. Tran-Cong, An improved dissipative particle dynamics scheme, Appl. Math. Model. 46 (2017) 602–617, https://doi.org/10.1016/j.apm.2017.01.086.
[26] S. Yaghoubi, E. Shirani, A.R. Pishevar, Improvement of dissipative particle dynamics method by taking into account the particle size, Sci. Iran. (2018), https://doi.org/10.24200/sci.2018.21042.
[27] E. Abu-Nada, Dissipative particle dynamics investigation of heat transfer mechanisms in Al 2 O 3 -water nanofluid, Int. J. Therm. Sci. 123 (2018) 58–72, https://doi.org/10.1016/j.ijthermalsci.2017.09.005.
[28] E. Abu-Nada, I. Pop, O. Mahian, A dissipative particle dynamics two-component nanofluid heat transfer model: application to natural convection, Int. J. Heat Mass Transf. 133 (2019) 1086–1098, https://doi.org/10.1016/j.ijheatmasstransfer.2018.12.151.
[29] E. Abu-Nada, Simulation of heat transfer enhancement in nanofluids using dissipative particle dynamics, Int. Commun. Heat Mass Transfer 85 (2017) 1–11, https://doi.org/10.1016/j.icheatmasstransfer.2017.04.008.
[30] K. Kara, A.N. Al-Khateeb, A. Alazzam, E. Abu-Nada, On the assessment of modeling combined convection heat transfer in nanofluids using dissipative particle dynamics, Int. J. Mech. Sci. 150 (2019) 561–575, https://doi.org/10.1016/j.ijmecsci.2018.10.062.
[31] J.B. Avalos, A.D. Mackie, Dissipative particle dynamics with energy conservation, EPL 40 (2) (1997) 141–146, https://doi.org/10.1209/epl/i1997-00436-6.
[32] P. Español, Dissipative particle dynamics with energy conservation, EPL 40 (6) (1997) 631–636, https://doi.org/10.1209/epl/i1997-00515-8.
[33] Z.-H. Cao, K. Luo, H.-L. Yi, H.-P. Tan, Energy conservative dissipative particle dynamics simulation of mixed convection in eccentric annulus, Int. J. Heat Mass Transf. 74 (2014) 60–76, https://doi.org/10.1016/j.ijheatmasstransfer.2014.03.022.
[34] Y.-X. Zhang, H.-L. Yi, H.-P. Tan, A dissipative particle dynamics algorithm for fluid-solid conjugate heat transfer, Int. J. Heat Mass Transf. 103 (2016) 555–563, https://doi.org/10.1016/j.ijheatmasstransfer.2016.07.094.
[35] T. Yamada, A. Kumar, Y. Asako, O.J. Gregory, M. Faghri, Forced convection heat transfer simulation using dissipative particle dynamics, Num. Heat Transf. A Appl. 60 (8) (2011) 651–665, https://doi.org/10.1080/10407782.2011.616847.
[36] Y. Xie, S. Chen, Numerical simulation of heat transfer in microchannel using energy conservative dissipative particle dynamics, Adv. Mech. Eng. 7 (3) (2015), https://doi.org/10.1177/1687814015571230 168781401557123.
[37] R. Qiao, P. He, Simulation of heat conduction in nanocomposite using energy-conserving dissipative particle dynamics, Mol. Simul. 33 (8) (2007) 677–683, https://doi.org/10.1080/08927020701286511.
[38] X. Fan, N. Phan-Thien, S. Chen, X. Wu, T. Yong Ng, Simulating flow of DNA suspension using dissipative particle dynamics, Phys. Fluids 18 (6) (2006) 63102, https://doi.org/10.1063/1.2206595.
[39] S. Yaghoubi, E. Shirani, A.R. Pishevar, Y. Afshar, New modified weight function for the dissipative force in the DPD method to increase the Schmidt number, EPL 110 (2) (2015) 24002, https://doi.org/10.1209/0295-5075/110/24002.
[40] E. Abu-Nada, Natural convection heat transfer simulation using energy conservative dissipative particle dynamics, Phys. Rev. E 81 (5) (2010), https://doi.org/10.1103/physreve.81.056704.
[41] X. Fan, N. Phan-Thien, N.T. Yong, X. Wu, D. Xu, Microchannel flow of a macromolecular suspension, Phys. Fluids 15 (1) (2003) 11–21, https://doi.org/10.1063/1.1522750.
[42] E. Abu-Nada, Application of dissipative particle dynamics to natural convection in differentially heated enclosures, Mol. Simul. 37 (2) (2011) 135–152, https://doi.org/10.1080/08927022.2010.533272.
[43] E. Abu-Nada, Dissipative particle dynamics simulation of natural convection using variable thermal properties, Int. Commun. Heat Mass Transfer 69 (2015) 84–93, https://doi.org/10.1016/j.icheatmasstransfer.2015.10.008.
[44] F. Pera, D. Dewitt, Introduction to Heat Transfer, John Wiley and Sons Inc., United States, 1985.